Characterization of the Sulfhydryl-Sensitive Site in the Enzyme Responsible for Hydrolysis of 2-Arachidonoyl-Glycerol in Rat Cerebellar Membranes

Susanna M. Saario,[1,*] Outi M.H. Salo,[1]
Tapio Nevalainen,[1] Antti Poso,[1] Jarmo T. Laitinen,[2]
Tomi Järvinen,[1] and Riku Niemi[1]
[1]Department of Pharmaceutical Chemistry and
[2]Department of Physiology
University of Kuopio
P.O. Box 1627
FIN-70211 Kuopio
Finland

Summary

We have previously reported that the endocannabinoid, 2-arachidonoyl-glycerol (2-AG), is hydrolyzed in rat cerebellar membranes by monoglyceride lipase (MGL)-like enzymatic activity. The present study shows that, like MGL, 2-AG-degrading enzymatic activity is sensitive to inhibition by sulfhydryl-specific reagents. Inhibition studies of this enzymatic activity by *N*-ethylmaleimide analogs revealed that analogs with bulky hydrophobic *N*-substitution were more potent inhibitors than hydrophilic or less bulky agents. Interestingly, the substrate analog *N*-arachidonylmaleimide was found to be the most potent inhibitor. A comparison model of MGL was constructed to get a view on the cysteine residues located near the binding site. These findings support our previous conclusion that the 2-AG-degrading enzymatic activity in rat cerebellar membranes corresponds to MGL or MGL-like enzyme and should facilitate further efforts to develop potent and more selective MGL inhibitors.

Introduction

2-arachidonoyl-glycerol (2-AG), a monoglyceride of arachidonic acid esterified at the *sn*-2 position, has been identified as an endogenous ligand for both CB1 and CB2 cannabinoid receptors [1, 2]. 2-AG has been reported to be the most abundant endocannabinoid in rat brain [1, 2] and is produced by neurons "on demand" and acts near the site of its synthesis. Formation of 2-AG is mediated by phospholipase C and diacylglycerol lipase [2]. Hydrolysis of 2-AG can be mediated either by monoglyceride lipase (MGL) or fatty acid amide hydrolase (FAAH), giving arachidonic acid and glycerol. Moreover, 2-AG can also be metabolized by COX-2 but not COX-1 to form prostaglandin 2-glyceryl esters [3].

Several studies have shown that 2-AG can be hydrolyzed by FAAH, which is also the enzyme responsible for the hydrolysis of the first identified endocannabinoid, *N*-arachidonoyl-ethanolamide [4–7]. However, more recent evidence supports the role of MGL, rather than FAAH, in the biological inactivation of 2-AG. Dinh and coworkers found that overexpression of MGL in rat cortical neurons diminished the accumulation of 2-AG

[8]. Recently, they reported that RNA interference-mediated silencing of MGL expression enhanced accumulation of 2-AG in HeLa cells [9]. Additionally, although serine hydrolase inhibitors phenylmethylsulphonyl fluoride (PMSF; IC_{50} 155 μM) and methyl arachidonylfluorophosphonate (MAFP; IC_{50} 2.2 nM) efficiently inhibited 2-AG degradation in rat cerebellar membranes, potent FAAH inhibitors, such as OL-53 and URB597, were found to be inactive in our previous study [10].

MGL is a serine hydrolase that assures complete hydrolysis of monoglycerides formed by the action of hormone-sensitive lipase and lipoprotein lipase [11]. MGL hydrolyzes medium- and long-chain fatty acids, such as palmitic acid, oleic acid, and arachidonic acid from the *sn*-2 position of monoglycerides, with the highest hydrolysis rate for arachidonic acid [12–14]. MGL mRNA has been found in rat adipose tissue, kidney, testis, brain, adrenal gland, lung, ovary, heart, and skeletal muscle [15]. Recently, Dinh et al. [8] reported that the mRNA for MGL is heterogeneously expressed in the rat brain with highest levels in cerebellum, cortex, and hippocampus. They also cloned MGL from a rat brain cDNA, which had 303 amino acids and a molecular weight of 33,367 Da. Karlsson et al. [15] also identified a lipase-specific catalytic triad (Ser122, Asp239, and His269) from mouse adipocyte MGL by site-directed mutagenesis experiments.

Previous studies have demonstrated that MGL is sensitive to inhibition by *p*-chloromercuribenzoic acid (*p*CMB), mercury chloride ($HgCl_2$), and *N*-ethylmaleimide (NEM) [16, 17], suggesting the presence of an essential sulfhydryl group(s) for catalytic activity. The aim of the present study was to characterize and localize a putative NEM-sensitive site on the enzyme by studying the sensitivity of MGL-like enzyme toward NEM analogs with varying *N*-substitution in rat cerebellar membrane preparation under previously described conditions [10]. Furthermore, in the absence of an experimentally determined structure of rat MGL, a comparison model for the enzyme was constructed to gain a better perspective on the 3D structural location of the putative MGL sulfhydryl groups. Finally, the sensitivity of MGL-like activity to the inhibition by *S*-nitrosothiols and other types of NO donors was investigated.
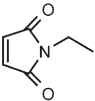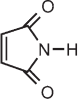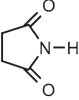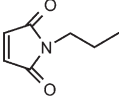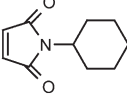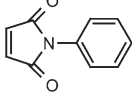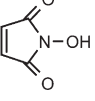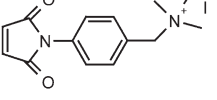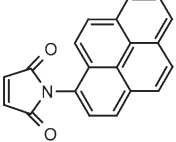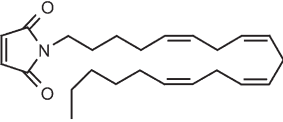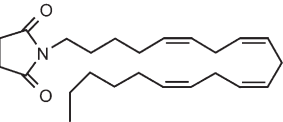
Results

In Vitro Studies

MGL-like activity in rat cerebellar membranes was inhibited by *p*CMB, $HgCl_2$, and NEM with IC_{50} values of 72 ± 8 μM, 42 ± 13 μM, and 53 ± 7 μM, respectively. The olefinic double bond in NEM is highly susceptible to nucleophilic attack by sulfhydryl group, which confers thiol reactivity to the molecule. Maleimide and succinimide, a ring-saturated analog of maleimide that is, thus, incapable of serving as a Michael acceptor, were studied for MGL inhibition activity to confirm the inhibition mechanism. It was observed that maleimide inhibited MGL-like activity with an IC_{50} value of 70 μM,

*Correspondence: susanna.saario@uku.fi

Table 1. IC$_{50}$ Values for the Inhibition of MGL-like Enzyme Activity in Rat Cerebellar Membranes by Various Maleimides and Succinimides

Compound	Structure	IC$_{50}$ value (μM)
NEM		53 ± 7
Maleimide		70 ± 6
Succinimide		No inhibition at 10 mM conc.
NPrM		53 ± 6
NCM		51 ± 6
NPhM		44 ± 6
NHM		413 ± 23
MBTA		68 ± 7
NPyrM		9.2 ± 0.8
NAM		0.14 ± 0.005
NAS		No inhibition at 1 mM conc.

Values represent mean ± SEM from three independent experiments performed in duplicate.

whereas succinimide did not show any inhibitory activity at 10 mM (Table 1). Eight N-alkyl/aryl maleimides of diverse hydrophobicity and size were examined for their ability to inhibit MGL-like enzyme in rat cerebellar membranes to gain more information on the NEM-sensitive site and to probe the enzyme structure (Table 1 and Figure 1). N-Phenylmaleimide (NPhM), N-cyclohex-ylmaleimide (NCM), N-propylmaleimide (NPrM), and 4-(N-maleimido)benzyl-α-trimethylammonium iodide (MBTA) inhibited 2-AG hydrolysis with almost identical IC$_{50}$ values (44 to 68 μM). N-hydroxymaleimide (NHM), which is a more hydrophilic compound than NEM, inhibited 2-AG degradation with an IC$_{50}$ value of 413 μM, which is approximately eight times less potent than
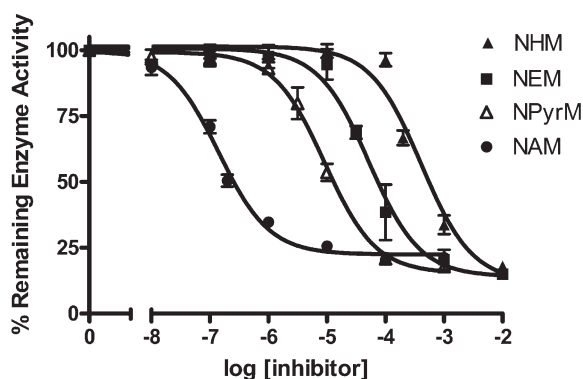
Figure 1. Inhibition of MGL-like Enzymatic Activity by NHM, NEM, NPyrM, and NAM in Rat Cerebellar Membranes

The remaining enzyme activity in the absence of inhibitors in the control samples was expressed as 100%. The enzyme activity in the control samples was 20 ± 1 nmol · min^{-1} · mg $protein^{-1}$ (mean ± SEM, n = 3). The data is represented as means ± SD of remaining enzyme activity (%) from three independent experiments performed in duplicate.

NEM. *N*-(1-pyrenyl)maleimide (NPyrM), a more lipophilic and bulkier compound compared to the above-mentioned maleimides, inhibited MGL-like activity with approximately six times higher potency (IC_{50} 9.2 μM) than NEM. Interestingly, *N*-arachidonylmaleimide (NAM), a compound having the most structural similarity to the natural MGL substrate 2-AG, was ∼380 times more potent than NEM with an IC_{50} value of 140 nM. To confirm that inhibition by NAM was due to the Michael addition reaction, *N*-arachidonylsuccinimide (NAS) was synthesized and tested against MGL-like activity at 1 mM concentration, and no inhibition was observed (Table 1). Additionally, the enzyme inhibition by NAM was not reversed by washing NAM-preincubated membranes three times with 1 ml of Tris-HCl buffer (50 mM [pH 7.4], 1 mM EDTA, and 0.5% BSA) prior to incubation (90 min at 25°C) with 2-AG. This finding further supports the formation of a covalent linkage between the enzyme and NAM. It is worth noting that the maximum inhibition achieved by any of these studied maleimides was ∼85%. The possible interactions of maleimide probes with the substrate (2-AG or 1[3]-AG) were excluded by confirming that the retention times of 2-AG or 1(3)-AG in the HPLC chromatograms showed no differences between the samples incubated with or without maleimides.

A previous study demonstrated that 2-AG is metabolized by COX-2 to prostaglandin glycerol esters [3]. Various COX-2 inhibitors, including nimesulide, indomethacin, acetylsalicylic acid, and ibuprofen, were tested at 100 μM in rat cerebellar membranes. However, no inhibition of 2-AG degradation was observed (data not shown). Furthermore, a possible role of COX-2 in 2-AG inactivation was excluded because the COX-2 inhibitors did not affect the sum of peak areas of 2-AG, 1(3)-AG, or arachidonic acid when compared to the control, which did not contain any COX-2 inhibitors, after 90 min of incubation.

The involvement of sulfhydryl-sensitive mechanisms in the enzymatic inactivation of 2-AG raises the possibility that cysteine residues could serve as potential targets for reversible modulation by *S*-nitrosylation. We investigated this possibility by treating rat cerebellar membranes with *S*-nitrosoglutathione (GSNO) and *S*-nitrosocysteine (CysNO), as well as the NO donor sodium nitroprusside (SNP). However, no effect on 2-AG degradation was observed by any of these compounds when tested up to 300–1000 μM concentrations (data not shown).

Molecular Modeling
When the first known MGL was sequenced, it was found to be distantly related to various microbial enzymes such as haloperoxidases, esterases, and lysophospholipases [15]. All these proteins, often even being seemingly nonhomologous with each other, share a similar tertiary fold, the so-called α/β hydrolase fold [18], which is also typical for many lipases [19]. Thus, modeling the core β sheet and the α helices packing against the sheet was relatively straightforward. Also, the catalytic triad Ser122-Asp239-His269 was well located because of the structural conservation of neighboring residues. Many lipases have been shown to have a helical segment, or lid, covering the active site [19]. In the crystal structure of chloroperoxidase L, for example, this lid is composed of four helices. Even though this part of the sequence is highly variable among the enzymes, the secondary structure prediction for the MGL sequence offers the possibility that MGL could have a lid comprised of four helices.

Karlsson and coworkers [15] have constructed a partial 3D model for MGL with the X-ray structure of bromoperoxidase A2 from *Streptomyces aureofaciens* as a template (pdb1bro) [20]. Similarly, they identified the catalytic triad, but the highly variable sequence region was obviously left out of the model.

According to the CYSPRED program [21], there are no disulfide bridges in MGL. Cysteines 32 and 55 are located in structurally conserved areas: Cys32 in the β2 strand and Cys55 at the beginning of the first helix (see Figure 2). Cysteines 201 and 208 are located in a highly variable region and are predicted to be at the end of the α6 helix and at the beginning of the α7 helix, respectively. Interestingly, Cys242 was found to be in a well-defined loop and in proximity to the catalytic triad (see Figure 3). Cys301 is situated at the end of the C terminus and, thus, left out of the model. A SYBYL MOLCAD surface (SYBYL v.6.9.2, Tripos Associates, Inc.) calculated for our model revealed a cavity at the bottom of which is the catalytic site. Cys208 is at the other end of this putative substrate binding cavity.

The ROBETTA server (see Experimental Procedures) produced five predicted rat MGL models that were comparable with each other by using chloroperoxidase F from *Pseudomonas fluorescens* (pdb1a8s) as a template for the largest part of the enzyme. In all these models, the catalytic triad and the cysteines are in the places comparable to our own model.

Also, the results from FUGUE (see Experimental Procedures) confirmed that our template choice and modeling alignment were reasonable. According to FUGUE, the haloperoxidase consensus structure was the sec-

```
                   *          20          *          40          *          60          *          80
                   EE EEE        EEEEEE           EEEEE       HHHHHHHHHHHH    EEEEE
Q8R431 : MPEASSPRRTPQNVPYQDLPHLVNADGQYLFCRYWKESGTPKALIFVSHGAGEHCGRYDELAQMLKRLDMLVFAHDHVGHGQSEGE : 86
1A88   : -------------------GTVTTSDGTNIFYKDWGERDG--LPVVFHHGWPLSADDWDNQMLFFLSHGYRVIAHDRRGHGRSD-Q : 64
                   EEE        EEEEEEEE         EEEEE      HHHHHHHHHHHH    EEEEE
                   β1              β2            β3          α1              β4


                    *          100          *          120 ▼         *          140          *          160          *
                    HHHHHHHHHHHHHHHHH       EEEEE HHH HHHHHHHHH       EEEE                        HHHHHHH
Q8R431 : RMVVSDFQVFVRDLLQHVNTVQKDYPEVPVFLLGHSMGG-AISILAAAEREITHFSGMILISPL--ILAN---------PESASTLK : 160
1A88   : PSTGHDMDTYAADVAALTEALDLRG----AVHIGHSTGGGEVARYVARAEIGRVAKAVLVSAVPPVMVKSDTNPDGLPLEVFDEFR : 146
                    HHHHHHHHHHHHH       EEEEE HHHHHHHHHH       EEEEE                        HHHHHHH
                    α2              β5    α3            β6              α4


                    *          180          *          200          *          220          *          240       * ▼
                    HHHHHHHHHH HHHHHHHHHHH     HHHHHHHHHHHHH     HHHHHHHHHHHHHHHHHHHHH         EEEEE        HH
Q8R431 : VLAAKLLNFVLPNISLGRIDSSVLS-RNKSEVDLYNSDPLICHAGVKVCFGIQLLNAVSRVERAMPRLTLPFLLLQGSADRLCDSK : 245
1A88   : AALAANRAQFYIDVPSGPFYGFNREGATVSQGLIDHWWLQGMMGAANAHYECIAAFSETDFTDDLKRIDVPVLVAHGTDDQVVPYA : 232
                    HHHHH HHHH  HHHH         HHHHHHHHHHHH     HHHHHHHHHHHHH         HHHHHH       EEEEEE
                    α5              β8            α6              α7          α8         β7


                    260          *          280 ▼         *          300          *
                    HHHHHHH       EEEEE        HHHHHHHHHHHHHHHHHHHHHH
Q8R431 : GAYLLMESSPSQDKTLKMYEGAYHVLHKELPEVTNSVLHEINTWVSHRIAVAGARCLP : 303
1A88   : DAAPKSAELLAN-ATLKSYEGLPHGMLSTHPEVLNPDLLAFVKS-------------- : 275
                    HHHHHHH       EEEEEE        HHHH HHHH HHHHHHH
                    α9              β8            α10  α11
```
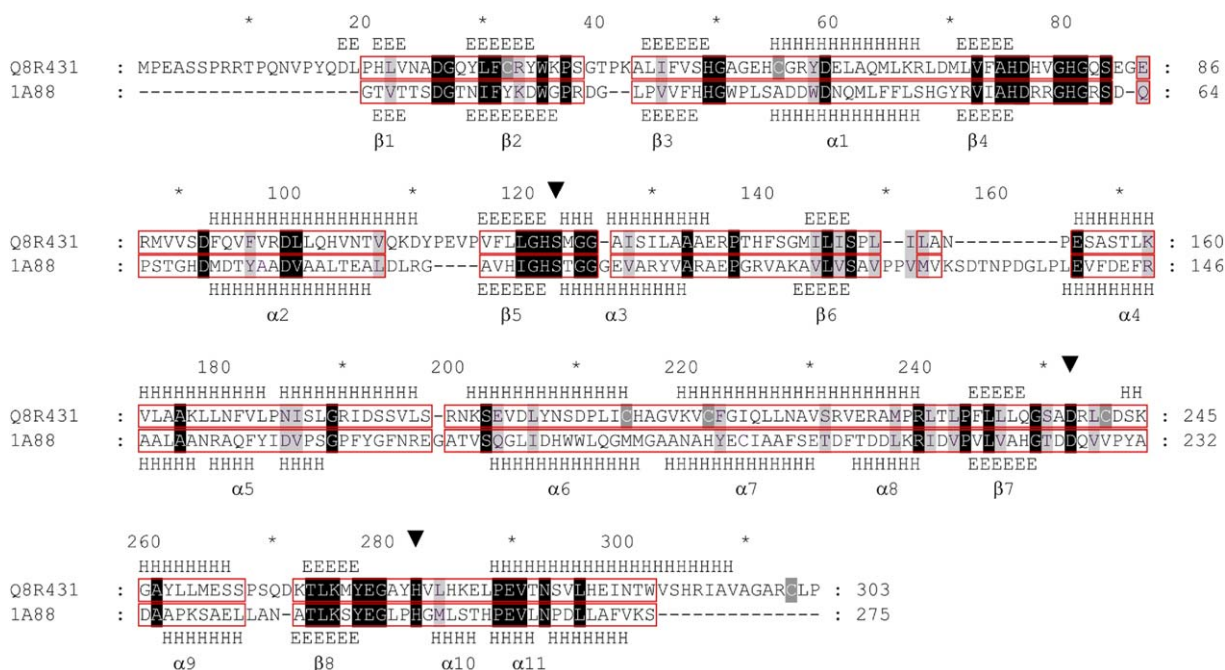
Figure 2. Modeling Alignment for the Sequences of Rat MGL and Chloroperoxidase L from *Streptomyces lividans*

Highly conserved residues are marked in black (identical residues) and light gray (conservatively replaceable residues). Cysteines in the rat MGL sequence (Q8R431) are highlighted with a dark gray background. Boxed regions denote the amino acid coordinates transferred from the chloroperoxidase X-ray structure (1A88) onto the MGL model. N and C termini were left out of the model. Predicted and experimentally determined secondary structures for rat MGL and chloroperoxidase L, respectively, are denoted by the letters E (β sheet) and H (α helix). β sheets and α helices are numbered according to the chloroperoxidase crystal structure. The residues of the catalytic triad are marked with an inverted triangle (▼).

ond best template (Z score, 23.65) after a bacterial carboxylesterase structure (pdb1r1d; Z score, 24.30), and both of these templates had a similar α/β hydrolase fold of the core enzyme. Only the variable lid area of the templates was somewhat different. Therefore, in the rough rat MGL models based on these templates, the cysteines were located at the same protein regions as in our model.
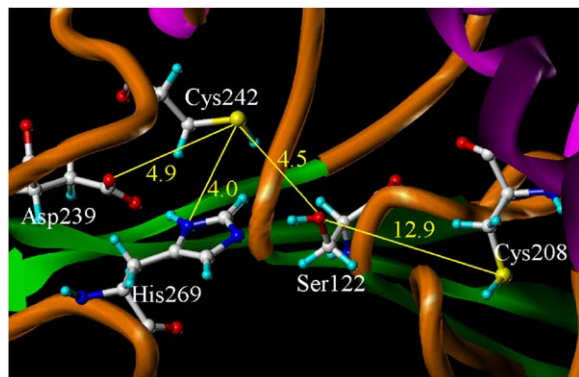

Figure 3. Catalytic Triad at the Rat MGL Model and the Cysteine Residues in Proximity of the Enzyme Active Site

Distances between the residues are presented in Ångströms. Color code: gray, carbon; red, oxygen; blue, nitrogen; cyan, hydrogen; yellow, sulfur; magenta, α helix; green, β strand; orange, loop/coil.

Discussion

Previous studies that have reported on the inhibition of MGL by *p*CMB, HgCl$_2$, and NEM suggest one or several essential sulfhydryl groups in MGL structure [22, 23]. In the present study, the above-mentioned sulfhydryl-specific compounds were shown to inhibit the enzymatic hydrolysis of 2-AG in rat cerebellar membranes. Moreover, the NEM-sensitive site on the MGL-like enzyme in rat cerebellar membranes was studied in more detail by using NEM analogs with varying *N*-substitution in order to determine how *N*-substitution alters the inhibitory activity of maleimides. NEM and its analogs have been broadly used for the modification of the cysteine sulfhydryl groups, which are generally considered to be the most reactive groups in a protein. NEM has also been shown to react with functional groups other than the SH group, for example the imidazole moiety of histidine [24]. However, those non-SH reactions effectively occur at only very high concentrations of NEM (100 mM) [25], which is ten times higher than the maximum concentration used in the present study (10 mM). The sulfhydryl moiety of cysteine interacts with the olefinic double bond of NEM to form a thioether [24]. This reaction is also known as Michael addition. In the present study, the lack of inhibition by succinimide strictly indicates that inhibition of MGL-like activity by maleimides occurs by the Michael addition reaction.

In the present study, MGL-like activity in rat cerebellar membranes was inhibited by maleimide, NEM,

NPhM, NCM, NPrM, and MBTA with no significant differences between their respecting IC_{50} values. However, hydrophilic NHM was approximately eight times less potent than the above-mentioned maleimides. NPyrM, the bulky and lipophilic maleimide, inhibited MGL-like activity with approximately six times lower IC_{50} value than NEM. *N*-Substitution in maleimides has been reported to have no effect on thiol reactivity per se [26]. However, the altered lipophilicity or steric hindrance caused by the *N*-linked maleimide side chains may alter their biological effects. The observation that increasing lipophilicity enhances the inhibitory activity of maleimides on MGL suggests that a NEM-sensitive site exists in a hydrophobic region of the enzyme.

There are six cysteine residues in the rat MGL cDNA [8]. Although the constructed MGL model is only a rough comparison model, the locations of the cysteines can be predicted with a reasonable accuracy. In the rat MGL sequence, Cys242 resides only three residues away from Asp239, and, therefore, it is not surprising to see it near the catalytic site in the 3D model. Assuming that the core of MGL would share a similar tertiary fold with the template, cysteines 32, 55, and 301 cannot locate near the active site. However, Cys201 and Cys208 are located in the structurally variable area and the positions of these residues can only be roughly predicted. Interestingly, the only cysteine residue of the chloroperoxidase template is in the sequence alignment located near Cys208 (Figure 2). According to the model, the sulfhydryl groups of two cysteines (Cys32 and Cys201) reside on the surface of the enzyme, whereas the sulfhydryl groups of Cys55, Cys208, and Cys242 are buried within the protein structure. Cysteines 208 and 242 are located in the proximity of the putative substrate binding site, suggesting a more lipophilic microenvironment for these sulfhydryl groups.

The substrate analog NAM was shown to be $\sim$380 times more potent than NEM as an inhibitor. The potency and structural similarity of NAM with 2-AG indicates that it binds to a sulfhydryl group within the substrate binding site. Additionally, the ring-saturated analog of NAM failed to inhibit MGL-like activity, proving that enzyme inhibition by NAM occurs through the Michael addition reaction. Moreover, the enzyme activity was not restored after washing NAM-preincubated membranes, indicating that the inhibition occurs through covalent modification of the enzyme. Hypothesized from the 3D model of rat MGL, either Cys242 or Cys208 could be modified by maleimides, thus leading to enzyme inactivation. However, the precise role of these cysteines should be confirmed experimentally, for example, by site-directed mutagenesis. The inhibition of MGL by maleimides could be due to simple steric hindrance, or it could cause a conformational change in the enzyme. The fact that the enzyme activity could not be abolished completely (remaining activity $\sim$15%) by any of these maleimides may be explained by the inhibition mechanism; maleimides bind to a cysteine located near to the catalytic triad not to the residues of the catalytic triad. The incomplete MGL inhibition by NEM was observed also by Sakurada and Noma [17] when they inhibited MGL by NEM (2 mM) in plasma membrane and cytosol fractions of rat adipocytes. The remaining enzyme activity was 25% and 15%, respectively [17]. However, the possibility that 2-AG is inactivated in rat cerebellar membranes by additional presently unknown enzymatic activity should also be taken into consideration.

Many enzymes with a reactive sulfhydryl group have been shown to be inhibited by NO reactive species [27]. In the current study, we determined the activity of the MGL-like enzyme in the presence of NO donors GSNO, CysNO, and SNP. However, no significant changes in the enzyme activity were shown by any of these NO donors. This result suggests that MGL-like activity is not under NO regulation, a finding in agreement with a previous study that demonstrated the inhibition of nitric oxide synthase by nitro L-arginine methyl ester and L-methylarginine had no effect on MGL activity in synaptoneurosomes [28].

Significance

The present study shows that maleimides with bulky hydrophobic *N*-substitution inhibit MGL-like enzyme in rat-cerebellar-membrane preparation more effectively than maleimides with hydrophilic or small hydrophobic *N*-substituted groups. In addition, the substrate analog NAM is a more potent inhibitor of MGL-like activity than the rigid NPyrM. The relatively high potency of NAM is most probably due to its structural similarity with the natural MGL substrate 2-AG. These results indicate that the critical cysteine residue lies within the lipophilic substrate binding pocket. According to the 3D model of rat MGL, cysteines 242 and 208 reside in close proximity to the putative 2-AG binding site, a finding that lets us hypothesize that the enzyme inhibition would occur because of alkylation of either of these cysteines, thus leading to steric hindrance of 2-AG binding at the active site. This intriguing hypothesis needs to be confirmed by further experiments, such as site-directed mutagenesis studies. Despite covalent attachment of maleimide compounds to a cysteine residue, the finding that MGL or MGL-like activity is effectively inhibited by NAM and maleimides with bulky hydrophobic *N*-substitution may facilitate further efforts to develop potent and selective MGL inhibitors. Such inhibitors could offer a rational therapeutic approach in treating certain pathological states, such as pain and neuroinflammation [29].

Experimental Procedures

Materials
2-AG was purchased from Cayman Chemical (Ann Arbor, Michigan). *N*-ethylmaleimide (NEM), BSA (essentially fatty acid free), glutathione, nimesulide, indomethacin, acetylsalicylic acid, and ibuprofen were purchased from Sigma (St. Louis, Missouri). Maleimide, *N*-cyclohexylmaleimide (NCM), *N*-hydroxymaleimide (NHM), *N*-phenylmaleimide (NPhM), *N*-propylmaleimide (NPrM), succinimide, *para*-chloromercuribenzoic acid (*p*CMB), $HgCl_2$, diethyl dicarboxylate (DEAD), and triphenylphosphine (Ph_3P) were purchased from Aldrich (Milwaukee, Wisconsin). 4-(*N*-maleimido)benzyl-α-trimethylammonium iodide (MBTA) and *N*-(1-pyrenyl) maleimide (NPyrM) were obtained from Toronto Research Chemicals, Inc. (North York, Ontario, Canada). Arachidonyl alcohol was purchased from Nu-Chek-Prep, Inc. (Elysian, Minnesota). L-Cysteine and sodium nitroprusside (SNP) were obtained from Merck (Darmstadt, Germany).

Animals and Preparation of Rat Cerebellar Membranes

Four-week-old male Wistar rats were used in these studies. All animal experiments were approved by the local ethics committee. The animals lived in a 12 hr light/12 hr dark cycle (lights on at 0700 hr) with water and food available ad libitum. The rats were decapitated 8 hr after lights on (1500 hr), and whole brains were removed, dipped in isopentane on dry ice, and stored at –80°C. Membranes were prepared as previously described [30–32]. Briefly, cerebella (minus brain stem) from eight animals were weighed and homogenized in nine volumes of ice-cold 0.32 M sucrose with a glass Teflon homogenizer. The crude homogenate was centrifuged at low speed (1,000 × g for 10 min at 4°C), and the pellet was discharged. The supernatant was centrifuged at high speed (100,000 × g for 10 min at 4°C). The pellet was resuspended in ice-cold deionized water and washed twice, and high-speed centrifugation was repeated. Finally, membranes were resuspended in 50 mM Tris-HCl (pH 7.4) with 1 mM EDTA and aliquoted for storage at –80°C. The protein concentration of the final preparation, measured by the Bradford method [33], was 15 mg/ml^{-1}.

Synthesis

The synthesis of *N*-arachidonylmaleimide (NAM) and *N*-arachidonylsuccinimide (NAS) was achieved by reacting arachidonyl alcohol with the appropriate imide, according to the modified Mitsunobu reaction [34].

N-Arachidonylmaleimide (NAM)

Ph$_3$P (70 mg, 0.27 mmol) was dissolved in dry THF. The resulting clear solution was cooled to –78°C. DEAD (47 mg, 0.27 mmol) was added, and a yellow reaction mixture formed. Arachidonyl alcohol (110 mg, 0.38 mmol) was added, and the reaction mixture was stirred for 5 min, after which maleimide (30 mg, 0.31 mmol) was added. The reaction mixture was kept at –78°C for 5 min after which it was removed to ambient temperature and stirred overnight. Progress of the reaction was monitored by TLC. The reaction mixture was concentrated under vacuum and purified by flash chromatography on silica gel with petroleum ether/ethyl acetate (7:1) as an eluent. After purification, 50 mg of *N*-arachidonylmaleimide was obtained (0.135 mmol, 44% yield, oil). ^{1}H NMR (CDCl$_3$): δ 0.89 (t, *J* = 6.8 Hz, 3H), 1.29–1.37 (m, 8H), 1.58–1.62 (m, 2H), 2.04–2.10 (m, 4H), 2.80–2.84 (m, 6H), 3.52 (t, *J* = 7.3 Hz, 2H), 5.30–5.42 (m, 8H), and 6.68 (s, 2H). ^{13}C NMR: δ 14.1, 22.6, 25.6 (3C), 26.7 (2C), 27.2, 28.1, 29.3, 31.5, 37.8, 127.6, 127.9, 128.2, 128.3, 128.4, 128.6, 129.5, 130.5, 134.1 (2C), and 170.2 (2C).

N-Arachidonylsuccinimide (NAS)

The synthesis of NAS was performed as described above, starting from 26 mg succinimide (0.26 mmol) and yielding 40 mg (0.11 mmol, 42%, oil). ^{1}H NMR (CDCl$_3$): δ 0.89 (t, *J* = 7.5 Hz, 3H), 1.26–1.40 (m, 8H), 1.56–1.62 (m, 2H), 2.03–2.11 (m, 4H), 2.69 (s, 4H), 2.79–2.85 (m, 6H), 3.51 (t, *J* = 6.9 Hz, 2H), and 5.30–5.43 (m, 8H). ^{13}C NMR: δ 14.1, 22.6, 25.6 (3C), 26.7, 26.8, 27.2, 27.3, 28.2 (2C), 29.3, 31.5, 38.8, 127.6, 127.9, 128.2, 128.3, 128.4, 128.6, 129.5, 130.5, and 177.2 (2C).

GSNO and CysNO

S-Nitrosoglutathione (GSNO) and *S*-nitrosocysteine (CysNO) were synthesized from their respective thiols with acidified NaNO$_2$, which was prepared by mixing 100 μl sodium nitrite (100 mM) with 100 μl HCl (150 mM) and then adding 100 μl reduced glutathione or L-cysteine (100 mM for both). Reactions were protected from light and allowed to proceed for 10 min at room temperature. Reaction mixtures were neutralized with 150 μl NaOH (100 mM) and immediately used in the experiments. Millipore-quality water was used throughout the study, and the assay buffer routinely contained 1 mM EDTA. The concentrations of RSNOs were determined by UV spectroscopy with previously published [35] values for the molar absorption coefficients (ε) and absorption maxima (λ$_{max}$).

Enzyme Assay

The experiments were carried out with preincubations (80 μl, 30 min at 25°C) containing 10 μg membrane protein, 44 mM Tris-HCl (pH 7.4), 0.9 mM EDTA, 0.5% (wt/vol) BSA, and 1.25% (vol/vol)

DMSO as a solvent for inhibitors. The preincubated membranes were kept at 0°C just prior to the experiments. The incubations (90 min at 25°C) were initiated by adding 40 μl of preincubated membrane cocktail, giving a final volume of 400 μl. The final volume contained 5 μg membrane protein, 54 mM Tris-HCl (pH 7.4), 1.1 mM EDTA, 100 mM NaCl, 5 mM MgCl$_2$, 0.5% (wt/vol) BSA, and 50 μM of 2-AG. At time points of 0 and 90 min, 100-μl samples were removed from incubation, acetonitrile (200 μl) was added to stop the enzymatic reaction, and pH of the samples were simultaneously decreased to 3.0 with phosphoric acid (added to acetonitrile) to stabilize 2-AG against acyl migration to 1(3)-AG. Samples were centrifuged at 23,700 × g for 4 min at room temperature prior to HPLC analysis of the supernatant. Under these conditions, the rate of arachidonic-acid formation was linear with respect to the membrane protein concentration up to 10 μg (data not shown) as well as to the 90 min incubation time (see [10]). During this incubation period, around 40% of the substrate was consumed.

HPLC Method

The analytical HPLC system consisted of a Merck Hitachi (Hitachi, Ltd., Tokyo) L-7100 pump, D-7000 interface module, L-7455 diode-array UV detector (190–800 nm, set at 211 nm), and L-7250 programmable autosampler. The separations were accomplished by a Zorbax SB-C18 endcapped reversed-phase precolumn (4.6 × 12.5 mm, 5 μm) and column (4.6 × 150 mm, 5 μm) (Agilent). The injection volume was 50 μl. A mobile phase mixture of 28% phosphate buffer (30 mM, pH 3.0) in acetonitrile was used at a flow rate of 2.0 ml/min^{-1}. Retention times were 5.8 min for 2-AG, 6.3 min for 1(3)-AG, and 10.2 min for arachidonic acid. The relative concentrations of 2-AG, 1(3)-AG, and arachidonic acid were determined by the corresponding peak areas. This was justified by the equivalence of response factors for the studied compounds and is supported by the observation that the sum of the peak areas was constant throughout the experiments.

Data Analyses

The results from the enzyme inhibition experiments are presented as mean ± SEM or mean ± SD of at least three independent experiments performed in duplicate. Data analyses for the dose-response curves were calculated as nonlinear regressions with GraphPad Prism 4.0 for Windows.

Molecular Modeling

The amino acid sequence of rat MGL was retrieved from the SWISS-PROT/TrEMBL database (Q8R431) [36], and a subsequent BLAST search [37] was made from the Protein Data Bank (PDB) [38] to find close homologs for the sequence. The X-ray structure of chloroperoxidase L (EC 1.11.1.10) from *Streptomyces lividans* (pdb1a88; chain A) [39] was chosen as the template for the process of comparative modeling. The rat MGL sequence was aligned with the template sequence, as well as with the sequences of bromoperoxidase A2 (EC 1.11.1.10; pdb1brt) [39], human MGL (TrEMBL: Q96AA5), and mouse MGL (TrEMBL: O35678) with the multiple sequence alignment program Clustal W 1.82 [40]. Additionally, secondary structures of rat MGL were predicted by the PSIPRED v 2.3 algorithm [41]. The multiple sequence alignment was then manually modified so that gaps were shifted to the loop regions, and the secondary structures of the template and rat MGL were closely matched (Figure 2). The CYSPRED [21] program, via the PredictProtein server [42], was used to predict disulfide bonds in the rat MGL structure.

The HOMOLOGY module of the InsightII v.2000 modeling package (Accelrys, Inc.) was used to extract the aligned coordinates (see Figure 2) from the chloroperoxidase X-ray structure and apply them to the MGL model. The loops for the model were selected from the PDB by a random loop search procedure implemented in InsightII. The coordinates of Gly100 and Gly172 in the chloroperoxidase structure were skipped, and the resulting gaps in the MGL model were repaired simply by joining the chain ends of the neighboring residues. Residue rotamers that severely clashed with other residues were changed into more favorable residues by utilizing the InsightII rotamer library.

Finally, the resulting comparison model was subjected to energy

minimization by the SYBYL (v. 6.9.2) modeling program as follows: (1) 50 iterations with the steepest descent method, keeping the catalytic triad and the backbone atoms of the secondary structures fixed; (2) 100 iterations with the conjugate gradient minimizer, keeping the same aggregate as in the first step; and (3) 200 iterations with the conjugate gradient minimizer, keeping only the catalytic triad as an aggregate. In SYBYL, the Kollman All-Atom force field with Kollman charges [43] was used for the minimization procedure. Subsequently, the hydroxyl group hydrogen atom of Ser122 was directed toward the NE2 nitrogen of His269.

For comparison, an automatic protein-structure prediction server ROBETTA [44, 45] was used to construct a 3D model of rat MGL. Also, the FUGUE program [46] that recognizes distant homologs by sequence-structure comparison was utilized to see if the choice of the template structure for rat MGL and the sequence alignment by the program were comparable with our modeling work.

Acknowledgments

References

1. Sugiura, T., Kondo, S., Sukagawa, A., Nakane, S., Shinoda, A., Itoh, K., Yamashita, A., and Waku, K. (1995). 2-Arachidonoyl-glycerol: a possible endogenous cannabinoid receptor ligand in brain. Biochem. Biophys. Res. Commun. *215*, 89–97.

2. Stella, N., Schweitzer, P., and Piomelli, D. (1997). A second endogenous cannabinoid that modulates long-term potentiation. Nature *388*, 773–778.

3. Kozak, K.R., Rowlinson, S.W., and Marnett, L.J. (2000). Oxygenation of the endocannabinoid, 2-arachidonylglycerol, to glyceryl prostaglandins by cyclooxygenase-2. J. Biol. Chem. *275*, 33744–33749.

4. Goparaju, S.K., Ueda, N., Yamaguchi, H., and Yamamoto, S. (1998). Anandamide amidohydrolase reacting with 2-arachidonoylglycerol, another cannabinoid receptor ligand. FEBS Lett. *422*, 69–73.

5. Di Marzo, V., Bisogno, T., Sugiura, T., Melck, D., and De Petrocellis, L. (1998). The novel endogenous cannabinoid 2-arachidonoylglycerol is inactivated by neuronal- and basophil-like cells: connections with anandamide. Biochem. J. *331*, 15–19.

6. Goparaju, S.K., Kurahashi, Y., Suzuki, H., Ueda, N., and Yamamoto, S. (1999). Anandamide amidohydrolase of porcine brain: cDNA cloning, functional expression and site-directed mutagenesis(1). Biochim. Biophys. Acta *1441*, 77–84.

7. Lang, W., Qin, C., Lin, S., Khanolkar, A.D., Goutopoulos, A., Fan, P., Abouzid, K., Meng, Z., Biegel, D., and Makriyannis, A. (1999). Substrate specificity and stereoselectivity of rat brain microsomal anandamide amidohydrolase. J. Med. Chem. *42*, 896–902.

8. Dinh, T.P., Carpenter, D., Leslie, F.M., Freund, T.F., Katona, I., Sensi, S.L., Kathuria, S., and Piomelli, D. (2002). Brain monoglyceride lipase participating in endocannabinoid inactivation. Proc. Natl. Acad. Sci. USA *99*, 10819–10824.

9. Dinh, T.P., Kathuria, S., and Piomelli, D. (2004). RNA interference suggests a primary role for monoacylglycerol lipase in the degradation of the endocannabinoid 2-arachidonoylglycerol. Mol. Pharmacol. *66*, 1260–1264.

10. Saario, S.M., Savinainen, J.R., Laitinen, J.T., Järvinen, T., and Niemi, R. (2004). Monoglyceride lipase-like enzymatic activity is responsible for hydrolysis of 2-arachidonoylglycerol in rat cerebellar membranes. Biochem. Pharmacol. *67*, 1381–1387.

11. Fredrikson, G., Tornqvist, H., and Belfrage, P. (1986). Hormone-sensitive lipase and monoacylglycerol lipase are both required for complete degradation of adipocyte triacylglycerol. Biochim. Biophys. Acta *876*, 288–293.

12. Okazaki, T., Sagawa, N., Okita, J.R., Bleasdale, J.E., MacDonald, P.C., and Johnston, J.M. (1981). Diacylglycerol metabolism and arachidonic acid release in human fetal membranes and decidua vera. J. Biol. Chem. *256*, 7316–7321.

13. Prescott, S.M., and Majerus, P.W. (1983). Characterization of 1,2-diacylglycerol hydrolysis in human platelets. Demonstration of an arachidonoyl-monoacylglycerol intermediate. J. Biol. Chem. *258*, 764–769.

14. Rindlisbacher, B., Reist, M., and Zahler, P. (1987). Diacylglycerol breakdown in plasma membranes of bovine chromaffin cells is a two-step mechanism mediated by a diacylglycerol lipase and a monoacylglycerol lipase. Biochim. Biophys. Acta *905*, 349–357.

15. Karlsson, M., Contreras, J.A., Hellman, U., Tornqvist, H., and Holm, C. (1997). cDNA cloning, tissue distribution, and identification of the catalytic triad of monoglyceride lipase. Evolutionary relationship to esterases, lysophospholipases, and haloperoxidases. J. Biol. Chem. *272*, 27218–27223.

16. Tornqvist, H., and Belfrage, P. (1976). Purification and some properties of a monoacylglycerol-hydrolyzing enzyme of rat adipose tissue. J. Biol. Chem. *251*, 813–819.

17. Sakurada, T., and Noma, A. (1981). Subcellular localization and some properties of monoacylglycerol lipase in rat adipocytes. J. Biochem. (Tokyo) *90*, 1413–1419.

18. Ollis, D.L., Cheah, E., Cygler, M., Dijkstra, B., Frolow, F., Franken, S.M., Harel, M., Remington, S.J., Silman, I., Schrag, J., et al. (1992). The alpha/beta hydrolase fold. Protein Eng. *5*, 197–211.

19. Jaeger, K.E., Dijkstra, B.W., and Reetz, M.T. (1999). Bacterial biocatalysts: molecular biology, three-dimensional structures, and biotechnological applications of lipases. Annu. Rev. Microbiol. *53*, 315–351.

20. Hecht, H.J., Sobek, H., Haag, T., Pfeifer, O., and van Pee, K.H. (1994). The metal-ion-free oxidoreductase from *Streptomyces aureofaciens* has an alpha/beta hydrolase fold. Nat. Struct. Biol. *1*, 532–537.

21. Fariselli, P., Riccobelli, P., and Casadio, R. (1999). Role of evolutionary information in predicting the disulfide-bonding state of cysteine in proteins. Proteins *36*, 340–346.

22. Tornqvist, H., and Belfrage, P. (1976). Purification and some properties of a monoacylglycerol-hydrolyzing enzyme of rat adipose tissue. J. Biol. Chem. *251*, 813–819.

23. Sakurada, T., and Noma, A. (1981). Subcellular localization and some properties of monoacylglycerol lipase in rat adipocytes. J. Biochem. (Tokyo) *90*, 1413–1419.

24. Smyth, D.G., Nagamatsu, A., and Fruton, J.S. (1960). Some reactions of N-ethylmaleimide. J. Am. Chem. *82*, 4600–4604.

25. Tirumalai, R.S., Pargellis, C.A., and Landy, A. (1996). Identification and characterization of the N-ethylmaleimide-sensitive site in lambda-integrase. J. Biol. Chem. *271*, 29599–29604.

26. Freed, B.M., Mozayeni, B., Lawrence, D.A., Wallach, F.R., and Lempert, N. (1986). Differential inhibition of human T-lymphocyte activation by maleimide probes. Cell. Immunol. *101*, 181–194.

27. Stamler, J.S., Lamas, S., and Fang, F.C. (2001). Nitrosylation: the prototypic redox-based signaling mechanism. Cell *106*, 675–683.

28. Farooqui, A.A., and Horrocks, L.A. (1997). Nitric oxide synthase inhibitors do not attenuate diacylglycerol or monoacylglycerol lipase activities in synaptoneurosomes. Neurochem. Res. *22*, 1265–1269.

29. Walter, L., Dinh, T., and Stella, N. (2004). ATP induces a rapid and pronounced increase in 2-arachidonoylglycerol production by astrocytes, a response limited by monoacylglycerol lipase. J. Neurosci. *24*, 8068–8074.

30. Lorenzen, A., Fuss, M., Vogt, H., and Schwabe, U. (1993). Measurement of guanine nucleotide-binding protein activation by A1 adenosine receptor agonists in bovine brain membranes: stimulation of guanosine-5′-O-(3-[35S]thio)triphosphate binding. Mol. Pharmacol. *44*, 115–123.

31. Kurkinen, K.M., Koistinaho, J., and Laitinen, J.T. (1997). [Gamma-35S]GTP autoradiography allows region-specific detection of muscarinic receptor-dependent G-protein activation in the chick optic tectum. Brain Res. *769*, 21–28.

32. Savinainen, J.R., Jarvinen, T., Laine, K., and Laitinen, J.T. (2001). Despite substantial degradation, 2-arachidonoylglycerol is a potent full efficacy agonist mediating CB(1) receptor-dependent G-protein activation in rat cerebellar membranes. Br. J. Pharmacol. *134*, 664–672.

33. Bradford, M.M. (1976). A rapid and sensitive method for the quantitation of microgram quantities of protein utilizing the principle of protein-dye binding. Anal. Biochem. *72*, 248–254.

34. Walker, M.A. (1995). A high yielding synthesis of N-alkyl maleimides using a novel modification of the Mitsunobu reaction. J. Org. Chem. *60*, 5352–5355.

35. Tullett, J.M., Rees, D.D., Shuker, D.E., and Gescher, A. (2001). Lack of correlation between the observed stability and pharmacological properties of S-nitroso derivatives of glutathione and cysteine-related peptides. Biochem. Pharmacol. *62*, 1239–1247.

36. Boeckmann, B., Bairoch, A., Apweiler, R., Blatter, M.C., Estreicher, A., Gasteiger, E., Martin, M.J., Michoud, K., O'Donovan, C., Phan, I., et al. (2003). The SWISS-PROT protein knowledgebase and its supplement TrEMBL in 2003. Nucleic Acids Res. *31*, 365–370.

37. Altschul, S.F., Madden, T.L., Schaffer, A.A., Zhang, J., Zhang, Z., Miller, W., and Lipman, D.J. (1997). Gapped BLAST and PSI-BLAST: a new generation of protein database search programs. Nucleic Acids Res. *25*, 3389–3402.

38. Berman, H.M., Battistuz, T., Bhat, T.N., Bluhm, W.F., Bourne, P.E., Burkhardt, K., Feng, Z., Gilliland, G.L., Iype, L., Jain, S., et al. (2002). The Protein Data Bank. Acta Crystallogr. D Biol. Crystallogr. *58*, 899–907.

39. Hofmann, B., Tolzer, S., Pelletier, I., Altenbuchner, J., van Pee, K.H., and Hecht, H.J. (1998). Structural investigation of the cofactor-free chloroperoxidases. J. Mol. Biol. *279*, 889–900.

40. Thompson, J.D., Higgins, D.G., and Gibson, T.J. (1994). CLUSTAL W: improving the sensitivity of progressive multiple sequence alignment through sequence weighting, position-specific gap penalties and weight matrix choice. Nucleic Acids Res. *22*, 4673–4680.

41. Jones, D.T. (1999). Protein secondary structure prediction based on position-specific scoring matrices. J. Mol. Biol. *292*, 195–202.

42. Rost, B., and Liu, J. (2003). The PredictProtein server. Nucleic Acids Res. *31*, 3300–3304.

43. Besler, B.H., Merz, K.M., and Kollman, P.A. (1990). Atomic charges derived from semiempirical methods. J. Comput. Chem. *11*, 431–439.

44. Kim, D.E., Chivian, D., and Baker, D. (2004). Protein structure prediction and analysis using the Robetta server. Nucleic Acids Res. *32*, W526–W531.

45. Chivian, D., Kim, D.E., Malmstrom, L., Bradley, P., Robertson, T., Murphy, P., Strauss, C.E., Bonneau, R., Rohl, C.A., and Baker, D. (2003). Automated prediction of CASP-5 structures using the Robetta server. Proteins Suppl. *53*, 524–533.

46. Shi, J., Blundell, T.L., and Mizuguchi, K. (2001). FUGUE: sequence-structure homology recognition using environment-specific substitution tables and structure-dependent gap penalties. J. Mol. Biol. *310*, 243–257.